Adaptive wing technology, aeroelasticity and flight stability: The lessons from natural flight

Dr. Pascual Marqués-Bruna, Faculty of Arts & Sciences, Edge Hill University,
St. Helen's Road, Ormskirk, L39 4QP, United Kingdom. marquesp@edgehill.ac.uk

Elena Spiridon, School of Natural Sciences and Psychology, Liverpool John Moores University,
Tom Reilly Building, Byrom Street, Liverpool, L3 3AF, United Kingdom. E.Spiridon@2008.ljmu.ac.uk

Abstract
This paper reviews adaptive wing morphology and biophysics observed in the natural world and the equivalent adaptive wing technology, aeroelasticity and flight stability principles used in aircraft design. Adaptive wing morphology in birds, including the Harris' hawk, Common swift, Steppe eagle and Barn swallow, provides excellent examples of aerodynamic and flight control effectiveness that inform the Aeronautical Engineer. The Harris' hawk and Common swift are gliding birds that change their wing and tail span according to gliding velocity. Inspired by the natural world, effective wing geometry is also modified in aircraft to adjust the aerodynamic load. Bird wings employ an automatic aeroelastic deflection of covert feathers that extend the range of flight configurations and maintain control authority in different flight regimes. Similarly, aircraft structures are not completely rigid and aeroelasticity is important in aircraft. In a Steppe eagle, the alula functions as a high-lift device analogous to the leading edge slats in aircraft wings that allow flight at high angles of attack and low airspeeds without stalling. It has also been suggested that the alula functions as a strake that triggers the development of a leading-edge vortex typical of aircraft delta wings. Sweep-back morphs the hand wing of birds into delta wings that produce lift-generating leading-edge-vortices. A biological high-lift flow-separation control mechanism exists in bird wings, whereby feathers pop up on the wing upper surface to stop the upstream proliferation of separated flow. The equivalent mechanism in aircraft is the self-activated moveable flap that augments maximum lift. Birds exploit stability in flight by morphing the wings and tail. The aeroelastic properties of tail streamers in a Barn swallow trigger an automatic deflection of the tail's leading edge. This deflection delays flow separation to higher angles of attack, generates higher aerodynamic lift and elicits greater manoeuvrability of the bird. The Aeronautical Engineer may optimise the handling, flying qualities and control of aircraft by mimicking the inherent adaptive morphology, aeroelasticity and flight stability principles observed in nature.

Keywords: Adaptive wing morphology, Aerodynamics, Biophysics, Bird flight, Engineering education.

Introduction

The adaptive wing morphology and biophysics observed in the natural world provide the foundation for the adaptive wing technology and flight control used in aircraft design. This paper reviews adaptive wing morphology in birds and biophysical concepts that the Aeronautical Engineer learns from the natural world. Bird wings are adapted to operate over a wide range of configurations **[1]**, ranging from the highly flexible kinematics of flapping to the constant geometry of gliding (Fig. 1). Birds are able to maintain control authority in different flight regimes during take-off, manoeuvring and landing when the wings operate at high angles of attack and in unsteady turbulent flow conditions. The wings rely on the aeroelastic deflection of covert feathers to extend the range of flight configurations **[2]**. Automatic aeroelastic wing and tail deformations compliment the active muscle-controlled changes in morphology and take different forms in nature. For example, the slotted primary feathers of a Griffon vulture (*Gyps fulvus*; Fig. 1) function as multi-planes that reduce induce drag by vertically spreading the wingtip vortices. Tail streamers in a Barn swallow (*Hirundo rustica*) act as automatic aeroelastic devices that deflect the tail's leading edge. Automatic deployment of covert feathers along the wing leading edge in a Steppe eagle (*Aquila nipalensis*) resemble aircraft leading-edge Krueger flaps **[1,3]**. The alula is a group of feathers at the wing leading edge that are attached to the wrist joint between the arm wing and hand wing. The alula has been described as a high-lift device that functions like leading edge slats in aircraft wings and allows flight at high angles of attack and low airspeeds without stalling **[4]**. Deflection of the alulae causes the boundary layer to remain attached at large angles of attack yielding up to 22% higher lift forces. Gliding Common swifts (*Apus apus*) generate stable leading edge vortices at angles of attack

of 5°–10° at realistic Reynolds numbers for swifts of $3.75 \times 10^3 – 37.5 \times 10^3$. The lift-generating leading-edge-vortex typical of delta wings **[5]** develops as a result of sweep-back of the hand wings by around 60°. In nature, birds change their wing span according to gliding velocity and exploit stability in flight by morphing the wings. In a fast glide, a shorter wing span reduces drag. However, birds increase wing span in a slow glide when coming in to land and swing the wings forward. This shifts the aerodynamic centre of pressure forward and causes a positive (head up) pitching moment that facilitates entry into a deep stall **[6]**.

Fig. 1. Wandering albatross (*Diomedea exulans*), Griffon vulture (*Gyps fulvus*) and Barn swallow (*Hirundo rustica*) in flight. *Photos: JJ Harrison; Luc Viatour; Thermos*.

Inspired by the natural world, adaptive wing technology in aircraft permits adjusting flow development to the variable aerodynamic load by modifying the effective wing geometry or activating flow control devices. The adaptive wing improves aerodynamic performance and structural design **[7]**. Any aircraft, military or civil transport, follows common flight procedures that include take off, climb, level flight and landing in changing freestream conditions. Fighter aircraft perform manoeuvres that require rapid changes in attitude and speed. Transport aircraft experience weight reduction during cruise due to fuel consumption which incurs changes in flow conditions and requires responsive flight control. Stanewsky **[7]** has emphasised that, to be effective in real aeronautical conditions, flow control must be adaptive to the changing flow characteristics within the aircraft flight envelope. Geometrical adjustments include variable wing sweep, deployment of slats and flaps (Fig. 2), variable leading or trailing edge camber, spanwise camber variations and many other systems that allow the wing to operate in off-design conditions **[8]**. Inviscid flow and boundary layer control is achieved using air-jet and sub-boundary layer vortex generators, suction or blowing to reduce viscous drag and prevent separation, passive cavity ventilation for shock control, to name a few **[9]**. High lift devices such as Gurney flaps and reverse-flow flaps augment the wing's maximum lift coefficient. An example of adaptive wing is that designed by FlexSys Inc. that features a variable-camber trailing edge that deflects up to ±10° and acts like a flap in a conventional wing. The wing also twists up to 1° per foot of span and the shape of the wing can be changed at a rate of 30°/s, making the wing suitable for gust alleviation. Another example is the Missio-Adaptive-Wing AFTI/F-111 experimental aircraft that uses variable leading and trailing edge camber to reduce drag **[9]**. In a quest to replicate the versatility of natural flight, the development of adaptive wing technology necessitates an interdisciplinary approach that includes aerodynamics, aeroelasticity, structures, and sensor and control engineering.

Fig. 2. Deployed high-lift devices in an RAAF Boeing C-17 Globemaster III (left) and McDonnell Douglas F/A-18 Hornet (right). *Photos: Marques Aviation Ltd; Jim Ross (NASA).*

Aeroelasticity concerns the interactions among inertial, elastic and aerodynamic forces **[8]**. As observed in nature, airplane structures are not completely rigid and aeroelasticity applies when structural deformations occur due to the aerodynamic forces. The additional aerodynamic forces augment the initial structural deformations that, in turn, increase the aerodynamic forces. These interactions may dissipate if equilibrium is reached or may diverge catastrophically due to resonance. Aeroelasticity is divided into *steady* (static) and *dynamic* **[8]**. Examples of dynamic aeroelastic phenomena include *flutter* and *dynamic response*. Flutter is a self-feeding, potentially destructive vibration mode. When a wing or rotor blade flutters, aerodynamic forces couple with the structure's natural mode of vibration and produce rapid periodic oscillations. When the energy input by the aerodynamic excitation in a cycle is larger than that dissipated by damping, the amplitude of vibration increases due to self-exciting oscillation. Dynamic response is the response of an aircraft to changes in airflow and atmospheric disturbances such as gusts or turbulence. An example of aeroelastic behaviour is found in the McDonnell Douglas F/A-18 Hornet experimental aircraft, configured as the X-53, which features an Active Aeroelastic Wing; Fig. 2. Active Aeroelastic Wing technology integrates wing aerodynamics, controls and structure to harness wing aeroelastic twist at high airspeed regimes and thus enhance aircraft performance. The active technology uses multiple leading and trailing edge control surfaces activated by a digital flight control system for subtle control of aeroelastic twist, while minimizing wing loading during manoeuvres, induced drag, aircraft structural weight and production costs **[8]**. For example, control surfaces such as tabs are deflected into the air stream to elicit wing twist and replace the reduced control generally associated with standard aileron reversal **[9]**. Energy from the air stream is employed to twist the wing with minimal control surface motion; thus, it is the wing itself that automatically creates most of the control forces. Using the concept of aeroelastic flexibility, the Active Aeroelastic Wing permits using a high-aspect-ratio, thin, swept wing suitable for the flight envelope and mission requirements of future fighter, bomber and transport aircraft.

The handling, flying qualities and control of aircraft are dictated by the inherent stability of the aircraft **[10]**. Static stability is the tendency of the aircraft to return to trimmed flight or equilibrium after a sudden disturbance caused by wind gusts, turbulence or a pilot-initiated action. Aircraft that are deliberately designed with limited aerodynamic stability rely on an electromechanical stability augmentation system **[8]**. Dynamic stability addresses the time history of the motion of the aircraft after a disturbance. Typically, the disturbance is gradually reduced over time due to damping. Optimum aerodynamic stability and control in pitch, roll and yaw are essential for both avian and aircraft flight. Despite the differences in size and operational Reynolds number, the adaptive flight stability mechanisms observed in the natural world continue to inspire the development of experimental aircraft.

Adaptive wing morphology and wing technology

Adaptive wing morphology and pitching equilibrium in a Harris' hawk (*Parabuteo unicinctus*; Fig. 3) was studied by Tucker **[6]**. The hawk glided freely in a wind tunnel using variations in wing span. When the hawk is flying in equilibrium, the sum of the pitching moments of the wings and tail and the angular acceleration about the pitching axis equal zero. To study pitching equilibrium, Tucker **[6]** located the centre of area of the wings using a planimeter and the *x* and *y* coordinates of about 300 points on wing projections from photographs. The center of area of the tail was located using a model that divides the projection of the tail into a central rectangle, two adjacent triangles and a segment of a circle at the rear of the tail. The area of the segment of a circle (S_{sc}) is obtained using eq. (1).

$$S_{sc} = c_t^2 tan^{-1}(b_{ts}/d) - db_{ts} \quad (1)$$

where, c_t is the tail chord, b_{ts} is the tail semi-span and d is the length of the rectangle. The center of area of the tail was found by integrating the mathematical functions for a rectangle (eq. 2), a triangle (eq. 3) and a segment of a circle (eq. 4).

$$x_{Sr} = -d/2 \quad (2)$$

$$x_{St} = -2d/3 \quad (3)$$

$$x_{Ssc} = -2b_{ts}^3/(3S_{sc}) \quad (4)$$

where, x_{Sr}, x_{St} and x_{Ssc} are the centers of area of the rectangle, triangle and segment of a circle, respectively. The location of the center of area for the combined wings and tail (x_T) is calculated using eq. (5).

$$x_T = (\sum x_{Si} S_i)/\sum S_i \quad (5)$$

where, i is the subscripts w, r, t or sc that refer to the wing, rectangle, triangle and segment of a circle, respectively **[6]**.

Fig. 3. Harris' Hawk (*Parabuteo unicinctus*).
Photos: Alan Vernon.

With increasing gliding velocity, the hawk decreased wing span and wing area, swept the wings backward and become therefore more streamlined (Fig. 4); whereby, lift is preserved but drag is curtailed. With decreasing gliding velocity, the hawk increased its wing span from 0.68 to 1.07 m and the center of area of the wings moved forward 0.09 wing chord lengths. This forward shift of the center of area produces a positive pitching moment that is opposed by the tail. However, the tail was observed to remain folded and only began to spread when wing span reached 87% of maximum **[6]**. It is common for gliding birds in

nature to spread their tails when the wings are almost fully extended. Spreading of the tail is assumed to generate a negative (head down) pitching moment that compensates for the forward movement of the wing center of area associated with extension of the wings. Spreading of the tail contributes approximately 10% of the hawk's total lift at maximum wing span and moves the center of area of the tail backwards, thus enhancing the compensatory negative pitching moment. Parabolic curves of gliding performance based on sinking velocity for three gliding birds are shown in Fig. 4. There is an optimum gliding velocity for minimum sinking velocity according to the adaptation of each bird species to remain airborne **[11]**.

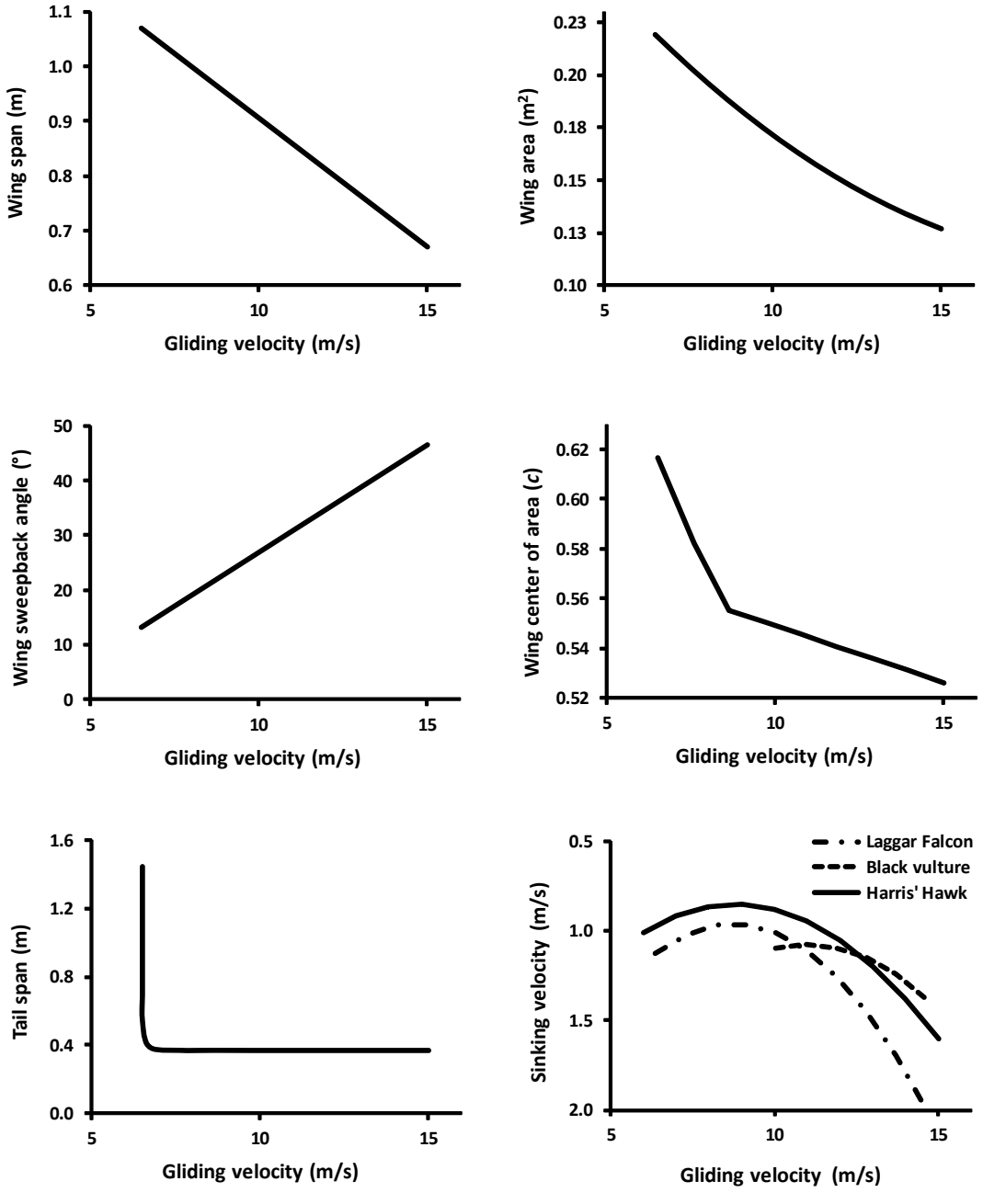

Fig. 4. Wing and tail configurations (Harris' hawk) and gliding performance (Laggar falcon, Black vulture and Harris' hawk) at different gliding velocities (adapted from [6,11]).

The aerodynamics of gliding flight of the Common swift were examined by Henningsson and Hedenström **[12]**. As observed in the Harris' hawk **[6]** (Fig. 4), a Common swift also adapts flight morphology and varies wing span (0.39 to 0.30 m), wing area (0.016 to 0.011 m^2) and tail span (0.09 to 0.04 m); according to gliding velocity (7 to 11 m/s, respectively). Sinking velocity also displayed a curvilinear relationship with gliding velocity. The minimum sinking velocity occurred at 8.1 m/s of gliding velocity, thus at a slightly lower gliding velocity than in the Laggar falcon and Harris' hawk (Fig. 4) **[11]**. Henningsson and Hedenström **[12]** used stereo digital particle image velocimetry to study the wake topology of the Common swift 8 to 11 wing chord lengths downstream the bird. Analogous to airplanes, the Common swift generates a pair of trailing wingtip vortices and a pair of tailtip vortices. Wake structure was used for the calculation of the circulation according to the *Lifting-line Theory* and the *Kutta-Joukowski Theorem* **[9]**. Both the wingtip and tailtip vortices were assumed to contribute to lift, thus total lift (L) was computed using eq. (6).

$$L = \rho U\left(b_{w,wake}\Gamma_w + b_{t,wake}\Gamma_t\right) \tag{6}$$

where, ρ is the air density, U is the airspeed, $b_{w,wake}$ is the average wingtip vortex wake span, Γ_w represents the average circulation of the wingtip vortex, $b_{t,wake}$ is the average tailtip vortex wake span and Γ_t symbolises the average circulation of the tailtip vortex. The Γ_w decreased in strength from 0.065 to 0.053, the standardised total lift coefficient changed from 0.81 to 0.43 and the total drag coefficient, based on wing and tail area, varied from 0.084 to 0.038; as gliding velocity augmented from 7 to 11 m/s, respectively **[12]**. The Laggar falcon, Black vulture and Harris' hawk are raptors adapted for soaring flight **[11]**. However, the Common swift is both in ecology and morphology different to most birds; it is an aerial insectivore and has wings with a short arm section and a very long hand section **[12]**. Flexion and sweep of the hand section allows high manoeuvrability for fast turning.

A biological high-lift flow-separation control mechanism exists in bird wings that resembles the self-activated moveable flaps used in aircraft that augment maximum lift **[2]**; Fig. 5. When flow separation starts to develop near the trailing edge of a wing, reverse flow that moves upstream occurs **[9]**. In birds, this reverse flow causes light feathers to pop up. The feathers prevent the proliferation of reversed flow towards the leading edge and delay flow separation yielding higher lift at lower flight speeds for a controlled landing **[7]**. The same principle observed in birds has been investigated in experimental aircraft as early as 1938. A Messerschmitt Me 109 fighter airplane was equipped with a piece of leather on the upper wing surface to simulate the feathers that cover the upper wing of birds **[2]**. Similarly, small moveable plastic sheets were installed on the upper surface near the trailing edge of the wing of a glider. Control of the reverse flow augmented the maximum lift coefficient and handling of the glider at high angles of attack. At low incidence, the moveable flap remains closed and does not cause any drag increments. However, as the angle of attack increases, flow separation near the trailing edge causes the flap to deploy automatically and self-adjust according to the aerodynamic forces and the weight of the flap. Thus, the flap provides passive flow control making active flap deployment by the aircraft flight control mechanism unnecessary **[7]**. The raised flaps reduce flow separation at high angles of attack and increase the lift coefficient of the airfoil by up to 13% **[2]**. However, some drag develops due to a small region of separated flow at the flap trailing edge. There is also a slight decrease in lift as the partially elevated flap changes the airfoil thickness near the trailing edge and causes the effective angle of attack of the airfoil to decrease. Bird wings counteract the problem of increased drag and reduced effective angle of attack by means of feather porosity and a jagged trailing edge and it has been suggested that aircraft wings should use the same principles **[2]**. Flap porosity can help equalize the static pressure between the upper and lower surfaces of the flap and a jagged trailing edge also facilitates an exchange of pressures. Because the reverse flow moves at slow velocity, compared to the freestream flow, it is essential that the movable flaps are very light and sensitive to weak reversed flows. In birds, light weight and sensitivity are achieved with feathers with a soft trailing edge. The effectiveness of self-activated movable flaps for aircraft has been examined using computational fluid dynamics **[2]**. A computational c-type mesh consisting of 1,000,000 nodes for a three-dimensional simulation was used. The computational domain included 6 chords upstream and 10 chords downstream of the flap configuration. The flap was modelled as a solid body that rotates about a hinge center (H) to a specific flap deflection angle (β), Fig. 5. Flap motion is determined by a balance of moments according to eq. (7).

$$\theta_S \frac{d_w^2 \beta}{d_w t^2} = -M_F(t) - M_G(t) \tag{7}$$

where, θ_S is the moment of inertia, d_w is the wall distance, t is time, M_F is the moment caused by fluid forces acting on the flap and M_G is the moment due to flap weight **[2]**. The two moments can be expressed in non-dimensional coefficient form; c_F and c_G, respectively. The $M_F(t)$ is a function of the difference between the static pressure on the upper (p_u) and lower (p_l) flap surfaces (eq. 8).

$$c_F = \frac{M_F}{\frac{1}{2}\,\rho\, c\, u_0^2\, b} = 2 \int_{r=0}^{l_F} \frac{r(p_u - p_l)}{\rho\, c^2\, u_0^2}\, dr \tag{8}$$

where, c is the chord length, u_0 is the inflow velocity, b is the wing span, r is the chordwise flap station and l_F is the flap length **[2]**. Self-activated movable flaps are a simple and cost-effective flow control mechanism that can be combined with active control devices such as conventional flaps. However, the use of these movable flow control tools is limited to subsonic flow regimes and non-swept wings.

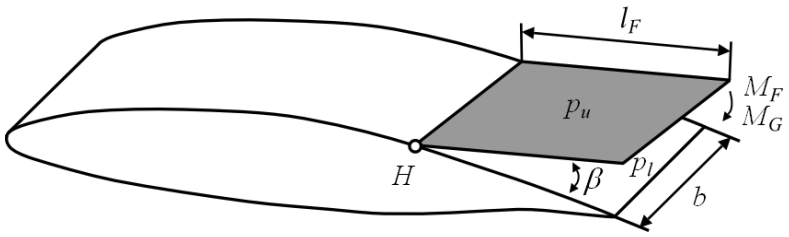

Fig. 5. Self-activated moveable flap.
Adapted from [2].

Like the pop up of feathers on the bird's wing or the elevated flaps in aircraft that control reverse flow, a device that also modifies airfoil thickness near the trailing edge is the adaptive bump control device **[8]**. However, Stanewsky **[7]** has estimated an annual reduction in fuel consumption of an A340-type aircraft of 2.11% at free stream Mach number of 0.84 when a well-adjusted adaptive bump control device is used. This is equivalent to a save in Cash Operating Costs (COC) of approximately 1.3%, according to eq. (9).

$$\Delta COC/COC = 0.49\Delta C_{D/D} + 1.9 \times 10^{-3}\, \Delta W + 0.113 \Delta mc/mc \tag{9}$$

where, C_D is the drag coefficient, W is the aircraft weight and mc/mc symbolises the increase in maintenance costs. Similarly, cuts in Direct Operating Costs of 0.8% associated with the use of bump control in an A3XX-type turbulent aircraft have been reported **[7]**. Unlike the adaptive bump control device, active flow control concepts have been proposed recently that do not easily find an equivalent aerodynamic mechanism in animal flight. Gaifutdinov and Il'inskii **[13]** suggested a method of designing separationless airfoils based on suction of a part of the upper surface external flow and jet injection from the airfoil trailing edge. This method of flow control considerably increases airfoil lift. However, this is an active method that requires energy expenditure for operation and explains why it is not found in natural flight, complimentary to moving flapping actuators, where flight economy play an essential part in the evolution of species **[6,11]**.

Carruthers *et al.* **[1]** filmed a Steppe eagle (Fig. 6) in free flight to study wing morphology, aeroelasticity and the functioning of covert feathers as the bird comes in to perch. The perching manoeuvre of the eagle comprises three phases: glide, pitch up and deep stall. As the Steppe eagle pitches up, a flap of covert feathers from the lower wing surface, that resembles the leading edge Krueger flaps in aircraft (Fig. 2), deploys passively **[1]**. Krueger flaps are high-lift devices that increase the wing's camber and maximum lift coefficient to prevent the aircraft from stalling at high angles of attack as it comes in to land **[7,9]**.

Fig. 6. Steppe eagle (*Aquila nipalensis*).
Photo: Wildpark Tripsdrill (Germany)

The tip of the bird's alula is also swept out automatically by the airflow as the eagle pitches up during the perching manoeuvre. It has been suggested **[1]** that the alula functions as a strake that triggers the development of a leading-edge vortex, typical of a delta wing, over the upper surface of the swept hand wing. The initial passive deployment of the alula by the airflow is thought to provide sensory feedback for the bird to fully deploy the alula. In the 1960s, M-wing planforms with adjustable leading edge flaps that match the geometry of the Steppe eagle's wings in the approach to perch, that is wings flexed into delta wings, were used in wind tunnel testing for the design of subsonic and transonic wing concepts **[1]**. M-wings exhibit unusual aerodynamic properties; in particular, a pitch up instability which is alleviated, nevertheless, by the use of leading edge flaps on the wing inner sections that correspond to the Steppe eagle's arm wings. In the Steppe eagle, the source of instability provided by the M shape of the wings is thought to facilitate the initial pitch up manoeuvre that precedes the deep stall. The initial pitch up rotation is immediately stabilised by the automatic aeroelastic deployment of the covert feathers that act as leading-edge flaps. During the deep stall, the bird adopts aerodynamics analogous to those of a cross-parachute. Modelled on nature, high-lift and flow control devices like those observed in a Steppe eagle represent advanced technology in aircraft. Kohlman **[14]** reports the flight test results of a modified Cessna 177 cardinal airplane. Improvements to the single engine light aircraft included installation of a wing with reduced surface area, Fowler flaps, Krueger flaps and spoilers. The modifications to the Cessna resulted in improved cruise performance, by increasing wing loading, and enhanced stall and roll control. Zero-lift drag was reduced by 14% and a maximum lift coefficient of 2.73 was attained. The light airplane was also more stable in gusty conditions and the spoilers enhanced roll control. Fowler flap deployment causes an aft displacement of the neutral point and enhances static stability in pitch **[10]**. The full-span Krueger leading-edge flap improves lift, yields about a 10-mph reduction in stall speed and makes the stall more docile and controllable; but causes no changes in longitudinal trim. Such experimental design features reported by Kohlman in the late 1970s are common in modern aircraft and closely resemble aerodynamics features found in birds.

An elongated tail in the Barn swallow (Fig. 1), in the form of narrow tail streamers, serves a mechanical and aerodynamic function. The aeroelastic properties of the tail streamers cause an automatic downward deflection of the tail's leading edge when the swallow spreads and lowers the tail. Flow separation on the upper surface is delayed to higher angles of attack. The tail achieves higher aerodynamic lift before reaching the stall and permits greater manoeuvrability and turns of smaller radii **[3]**. As per a Barn swallow flying in its natural environment, modern fighter aircraft require high performance capabilities for flight at high angles of attack during rapid manoeuvres under adverse unsteady flow conditions **[15]**. In particular, unusual accelerations and angular rates require high manoeuvrability, agility and advanced dynamic stability. Using recent developments in dynamics and control of flexible aircraft, Tuzcu **[16]** bridges the gap between two separate disciplines of aircraft stability; namely, flight dynamics and aeroelasticity. In the flight dynamics approach, nonlinear ordinary differential equations are linearized about a steady trim. In contrast, aeroelasticity is concerned with restrained flexible aircraft, such as an

airfoil section supported by springs or a wing fixed at its root but deformed by aerodynamic forces, in which the motion may be described using partial differential equations. Thus, the work of Tuzcu **[16]** combines flight dynamics and aeroelasticity and permits a broader approach to the traditional concept of flight stability **[10]**, as well as a method for the prediction of divergence and flutter. The foundations of combined flight dynamics and aeroelasticity can be traced back to natural flight.

Conclusion

Principles of adaptive wing morphology and biophysics derived from the natural world help the Aeronautical Engineer devise equivalent adaptive wing technology for the design of aircraft. Unparalleled examples of adaptive wing morphology, aeroelasticity and flight stability are found in the Harris' hawk, Common swift, Steppe eagle and Barn swallow. The Harris' hawk and Common swift morph their wings and tail during gliding to adjust aerodynamic load and reduce drag. Automatic aeroelastic deflection of covert feathers allows birds to extend the range of flight regimes. Flexible aeroelastic structures are also used in aircraft to harness aerodynamic twist and minimize wing loading during manoeuvres. The alula in a Steppe eagle is an interesting high-lift device that resembles the leading edge slats in aircraft wings for flight at high angles of attack. The alula may also function as a strake that generates a leading-edge vortex, typical of aircraft delta wings. Wing sweep-back in a Common swift morphs the wing into a delta wing that produces a leading-edge vortex. In birds, feathers pop up on the wing upper surface and prevent the proliferation of separated flow. Self-activated moveable flaps in aircraft serve the same flow-separation control function. The aeroelastic properties of tail streamers in a Barn swallow incur an automatic deflection of the tail's leading edge and the bird achieves higher lift and manoeuvrability. The inherent biophysical principles observed in nature are an unsurpassed reference in the design of adaptive wing technology for aircraft.

Acknowledgement

The authors would like to acknowledge the financial support provided by Edge Hill University for this project.

Authors' biographies

Dr Pascual Marqués obtained his MPhil from Brunel University in 1998 and his PhD from Liverpool John Moores University in 2005, both in Biomechanics. Dr Marqués has been a Lecturer at The University of Exeter, Brunel University and South Bank University and he is currently at Edge Hill University in the United Kingdom. His research involves numerical modelling of aerodynamics for applications in Engineering using CAD, MATLAB and AeroFoilEngineering software. Recent projects include the optimization of aerodynamic stability in ski jumping and wing design for sports cars.

Elena Spiridon is a Lecturer in Psychology at Liverpool John Moores University and was formerly a lecturer at Edge Hill University. Elena obtained her BSc (Hons) Psychology (First Class degree classification) from Lancaster University in 2007. She was granted the 2007 GBR British Psychological Society Award for the highest average University mark. Elena is a member of the REFLECT project research team within the 7th Framework Programme (FP7) funded by the European Commission. Her research interest is in the development of a prototype biocybernetic system that measures affective-motivational states via psychophysiology and provides feedback to the user in real-time.

References

1. Carruthers AC, Thomas ALR and Taylor GK. (2007). Automatic aeroelastic devices in the wings of a steppe eagle *Aquila nipalensis*. *The Journal of Experimental Biology*. ***210***(23): 4136-4149.
2. Schatz M, Knacke T, Thiele F, Meyer R, Hage W and Bechert DW. (2004). Separation control by self-activated movable flaps. *42nd AIAA Aerospace Sciences Meeting and Exhibit*. 5-8 January, Reno, NV. Pp. 1-12.
3. Norberg RA. (1994). Swallow tail streamer is a mechanical device for self deflection of tail leading edge, enhancing aerodynamic efficiency and flight manoeuvrability. *Proceedings of the Royal Society of London. Series B: Biological Sciences*. ***257***(1350): 227-233.
4. Meseguer J, Franchini S, Perez-Grande I and Sanz IL. (2005). On the aerodynamics of leading-edge high-lift devices of avian wings. *Proceedings of the Institution of Mechanical Engineers, Part G, Journal of Aerospace Engineering*. ***219***(1): 63-68.

5. Lentink D, Müller UK, Stamhuis EJ, de Kat R, van Gestel W, Veldhuis LL, Henningsson P, Hedenström A, Videler JJ and van Leeuwen JL. (2007). How swifts control their glide performance with morphing wings. *Nature*. ***446***(7139): 1082-1085.
6. Tucker VA. (1992). Pitching equilibrium, wing span and tail span in a gliding Harris Hawk, *Parabuteo unicinctus*. *The Journal of Experimental Biology*. ***165***(1): 21-41.
7. Stanewsky E. (2000). Aerodynamic benefits of adaptive wing technology. *Aerospace Science and Technology*. ***4***(7): 439-452.
8. Wright JR and Cooper JE. (2007). *Introduction to aircraft aeroelasticity and loads*. John Wiley & Sons. London.
9. Bertin JJ. (2002). *Aerodynamics for engineers*. Prentice Hall. New Jersey.
10. Nelson RC. (1998). *Flight stability and automatic control*. McGraw Hill. New York.
11. Tucker VA and Heine C. (1990). Aerodynamics of gliding flight in a Karris' Hawk, *Parabuteo unicinctus*. *The Journal of Experimental Biology*. ***149***(1): 469-489.
12. Henningsson P and Hedenström A. (2011). Aerodynamics of gliding flight in common swifts. *The Journal of Experimental Biology*. ***214***(3): 382-393.
13. Gaifutdinov RA and Il'inskii NB. (2008). Designing wing airfoils with active flow controls. *Fluid Dynamics*. ***43***(4): 547-554.
14. Kohlman DL. (1979). Flight test results for an advanced technology light airplane. *Journal of Aircraft*. ***16***(4): 250-255.
15. Altun M and Iyigun I. (2004). Dynamic stability derivatives of a maneuvering combat aircraft model. *Journal of Aeronautics and Space Technologies*. ***1***(3): 19-27.
16. Tuzcu I. (2008). On the stability of flexible aircraft. *Aerospace Science and Technology*. ***12***(5): 376–384.